

Contactless Excitation of MEMS Resonant Sensors by Electromagnetic Driving

M. Baù*, V. Ferrari, D. Marioli

Department of Electronics for Automation, University of Brescia

*M. Baù: Via Branze, 38-25123 Brescia (Italy), marco.bau@ing.unibs.it

Abstract: A contactless electromagnetic principle for the excitation of mechanical vibrations in resonant structures has been investigated. The principle relies on no specific magnetic property of the resonator except electrical conductivity and can be adopted for employing the structures as resonant sensors for measurements either in environments not compliant with the requirements of active electronics or in limited accessibility environments. An external coil is employed as an excitation source which inductively couples to the conductive surface of the resonator or to a secondary coil connected to conductive paths on the resonant structure. Exploiting the interaction of the induced currents with AC or DC magnetic fields, Lorentz forces are generated which can set the resonator into vibration. Preliminary tests on miniaturized resonators have been performed, namely cantilevers and clamped-clamped beams. The principle has been subsequently implemented in the design of MEMS resonators. Experimental verifications have shown the possibility of contactless exciting microresonators over short-range distances.

Keywords: Contactless interrogation, MEMS resonators, electromagnetic excitation.

1. Introduction

This work investigates a principle based on electromagnetic techniques for the contactless excitation of mechanical resonances in structures to be used as sensors for a large variety of physical or chemical quantities. Contactless excitation of mechanical resonators is attractive for applications that do not allow for cabled solutions, e.g. for in-package or in-body measurements. The possibility of using completely passive structures is also attractive for operations in harsh environments incompatible with active electronics e.g. at high temperature. In this context the use of the resonant principle seems effective because the resonance frequency does not depend on the particular

interrogation technique adopted and because of its intrinsic robustness.

The proposed approach avoids the use of magnetic films deposited on the structure because, when applied to MEMS (Micro Electro-Mechanical Systems) resonators, it requires dedicated post-fabrication steps, usually not compliant with traditional micromachining processes [1]. The investigated principle requires the structures only to be electrically conductive in a suitable frequency range, without having any specific magnetic property. The excitation of mechanical resonances in nonmagnetic structures can be obtained by exploiting the interaction between an AC current flowing either in the microstructure [2, 3], or in a proximate coil [4-6] and a time-varying or static magnetic field.

As a first step in the research activity, the excitation of conductive miniaturized structures has been addressed. The investigated technique relies on the generation on the conductive surface of the resonator of an eddy-current density by means of an external AC magnetic field at frequency f_e . The interaction of the eddy-current density with the same magnetic field generates Lorentz forces at frequency $2f_e$ that can set the structure into vibration. The principle has been demonstrated to be effective when applied to different typologies of resonators, namely cantilever beams and clamped-clamped beams [7].

The application of the electromagnetic excitation principle to MEMS structures has required the analysis of the effects of the downscaling of the dimensions, that is the reduction of the forces acting on the microstructures and the increase of the mechanical stiffness. To this purpose, simulations and dedicated strategies have been investigated to improve the effectiveness of the contactless excitation principle and implemented in design of a set of MEMS devices. In particular, the interaction between an external static magnetic field and an AC current contactless induced in predefined paths on the microstructure has been exploited.

2. The contactless electromagnetic excitation principle

Figure 1 shows a simplified schematic diagram of the principle of contactless electromagnetic excitation. A resonator with a conductive surface layer is placed in the region where a magnetic field is generated by a coil. The winding of the coil is driven by a sinusoidal time-varying current $I_e(t)$ at frequency f_e to generate a sinusoidal magnetic field $B_e(t)$.

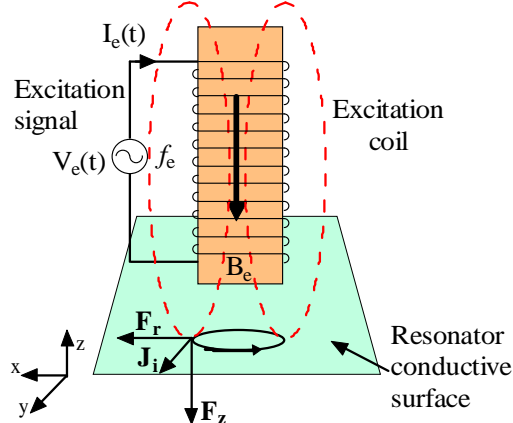


Figure 1. Schematic diagram of the excitation principle.

Because of the axial symmetry of the configuration, the field B_e is composed of a radial component B_{er} and a vertical component B_{ez} . The time variation of the flux of B_{ez} through the conductive surface of the resonator generates an electromotive force $V_e(t)$. The electromotive force is responsible for the circulation of an eddy current density J_i in the conductive layer. Due to the geometry, J_i has only in-plane component and the following expression can be assumed:

$$J_i(t) = J_0(f_e) \sin(2\pi f_e t + \varphi) \quad (1)$$

where both the amplitude J_0 and the phase φ are dependent on the electrical impedance $Z(f) = |Z(f)|e^{j\varphi(f)}$ of the conductive layer. It must be observed that at the frequency of interest in the present study (that is tens of kilohertz) the electromagnetic penetration depth in common conducting material is larger than the adopted conductive layer thickness. As a consequence, the eddy-current density can be assumed to be uniform throughout the thickness of the conductive layer. The eddy-current density

interacts with the overall magnetic field and a Lorentz force per unit of volume is generated which acts on the resonator. In particular, observing that the force in the z direction is given by the interaction of J_i with the radial component B_{er} , the following expression for the vertical force F_z can be derived:

$$F_z = (1/2)J_0(f_e)B_{er} [\sin(\varphi) + \sin(2\pi 2f_e t + \varphi)] \quad (2)$$

It can be observed that the force F_z is composed of a sinusoidal term at twice the excitation frequency f_e , proportional to the time-varying component of the external field plus a DC term dependent on the phase of the electrical impedance of the conductive layer. According to (2), to excite a vibration mode of a resonator at frequency f_r , the excitation coil must be driven at frequency f_e so that $f_r = 2f_e$ [7].

Alternatively, the current density J_i can interact with a static magnetic field B_0 generated by either a DC current in the central winding or by a proper arrangement of external magnets having at the surface of the resonator a radial component B_{0r} . In this case the Lorentz magnetic forces can be written as:

$$F_z = (1/2)J_0(f_e)[B_{er} \sin(\varphi) + 2B_{0r} \sin(2\pi f_e t + \varphi)] \quad (3)$$

From (3) it can be observed that the AC component of the force is proportional to the static component of the magnetic field, while the DC term is dependent on the amplitude of the AC component. According to (3), to excite a vibration mode of a resonator at frequency f_r , the excitation coil must be driven at the same frequency $f_r = f_e$.

As it will be demonstrated in the following paragraph, the electrical behavior of the resonator surface at the working frequencies of interest, is predominantly resistive. As a consequence, both in (2) and (3) the phase φ can be assumed to be nearly zero and no significant DC term is expected in the force F_z .

3. Application of the excitation principle to miniaturized resonators

3.1 Simulations on the excitation principle

In the first stage of the activity dedicated to millimeter-size structures, COMSOL

Multiphysics has been adopted to verify the theory of the excitation principle previously explained. Without the aim of analyzing any specific configuration, the simulations have been run to investigate the effects of the geometric dimensions of the resonator and of the coil on the forces acting on the resonator.

To this purpose, the simulated configuration of the system has been reduced to a geometry with axial symmetry, modeling the resonator as a conductive disc with thickness t and radius R_d . The coil has been modeled as a cylinder with radius R_c and length l , while the distance between the bottom surface of the coil and the top surface of the disc has been set to h . The current supplied to the coil has been modeled by a surface current J_s . Figure 2 shows the simulated geometry and the results of an AC electromagnetic simulation. In particular the streamline plot represents the lines of the magnetic field, while the colormap plot represents the distribution of the induced eddy currents in the resonator.

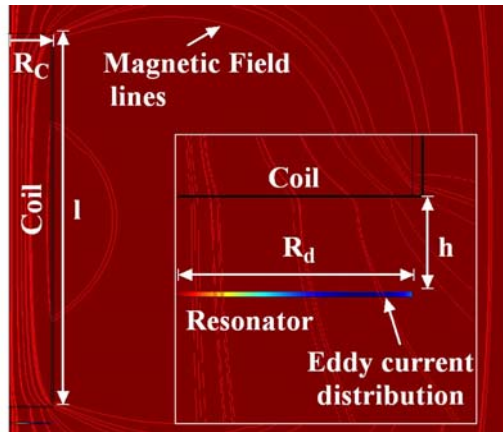


Figure 2. Schematic diagram of the simulated geometry.

The force F_z per unit of volume along the z direction acting on the resonator has been calculated by properly implementing equation (2). To compare the effects of the geometry on the electromagnetic force, the following parameter f_{norm} has been defined:

$$f_{norm} = \frac{1}{V} \int_V F_z dV \quad (4)$$

which represents the total force in the z -direction acting on the resonator, normalized to the volume V of the resonator.

Figure 3 shows the value of $|f_{norm}|$ for different values of the radius R_d of the disc, while the radius of the coil R_c is set to 2.5 mm and the distance h is 5 mm. It can be observed that the parameter $|f_{norm}|$ has a maximum for a specific value of R_d showing that for a given coil radius, there exists a narrow range of the dimensions of the resonator for which the applied force is maximized.

The impedance $Z(f)$ associated to the eddy-current closed paths on the conductive layer as a function of the frequency has also been investigated. The impedance is assumed to be modelled by a resistance R in series with a reactance X , both of which may depend on frequency. The simulation is based on an energetic method to evaluate both R and X . Figure 4 shows the resistance R and the reactance X in the frequency range [100 Hz–100 kHz]. As it can be argued, the electrical behavior of the disc is predominantly resistive, supporting the hypothesis of no significant DC component in the expression of the force.

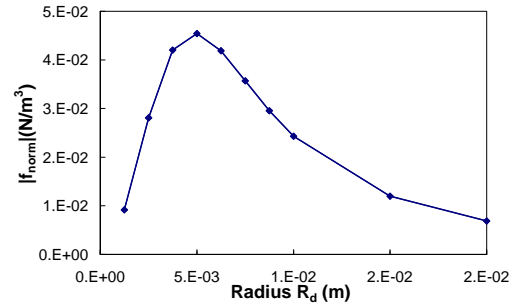


Figure 3. $|f_{norm}|$ versus the radius R_d of the disc.

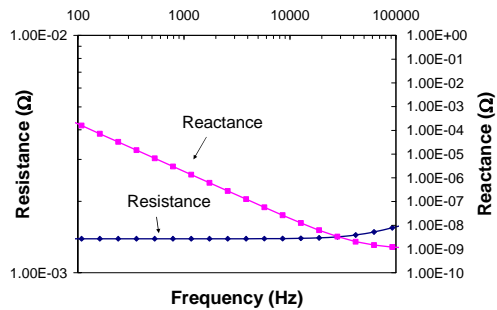


Figure 4. Resistance R and reactance X of the disc versus frequency.

3.2 Experimental results on miniaturize resonators

The principle has been applied to a variety of mechanical structures, namely metallic cantilevers and clamped-clamped beams have been used as resonators. The induced vibrations have been detected by a contactless optical system previously developed for the characterization of resonators vibrating in out-of-plane mode [7].

The system, shown in Figure 5, can measure the frequency response of the resonator under forced excitation conditions by a technique similar to synchronous demodulation with lock-in detection.

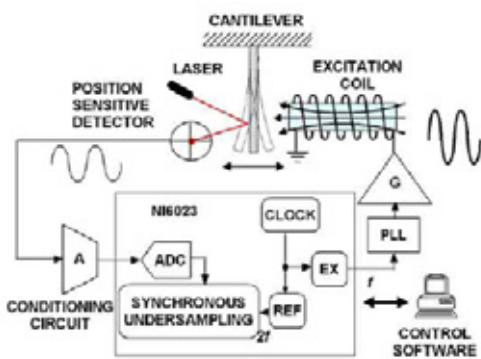


Figure 5. Schematic diagram of the experimental setup.

As an example, the results on an aluminum ($\sigma=2.326 \times 10^7$ S/m, $E=69 \times 10^9$ Pa, $\rho= 2730$ kg/m³) clamped-clamped beam of dimensions 17 x 1.4 x 0.1 mm excited at a distance of 5 mm and with a supplied current in the coil of 26 mA rms are reported. The coil has a diameter of 2 mm and length of 40 mm.

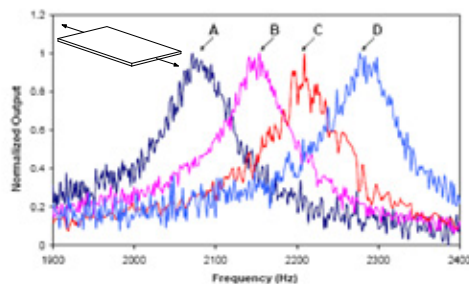


Figure 6. Normalized frequency responses for the clamped-clamped beam.

The resonator, shown in the inset of Figure 6, can be tuned to different resonant frequencies by

applying a mechanical axial tension. Figure 6 shows the measured frequency responses for increasing values of the axial tension applied (from curve A to curve D). As expected, when the axial tension is increased a corresponding up-shift of the frequency is observed.

4. Application of the excitation principle to MEMS resonators

4.1 MEMS Design

In the second stage of the activity the possibility of applying the excitation principle to MEMS devices has been investigated. From the electromagnetic point view, the downscaling of the dimensions of the resonators implies a reduction of the total flux linked to the structures with a corresponding decrease of the induced eddy-current density and of the total Lorentz force. On the other hand, from the mechanical point of view an increase in the mechanical stiffness of the resonator is expected. To counteract such effects and obtain suitable Lorentz forces to set the resonator into vibration, the proposed approach for cantilever resonators is shown in Figure 7.

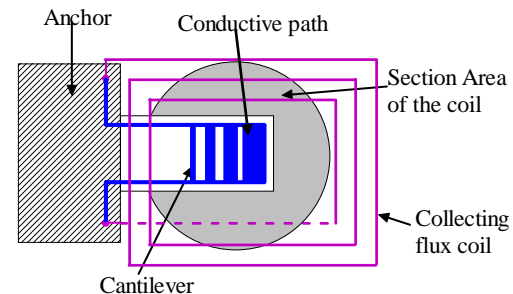


Figure 7. Schematic diagram of the proposed solution for MEMS cantilevers.

On the surface of the cantilever a conductive path has been placed, which has two purposes. Firstly, the conductive path is connected to a collecting flux coil which allows to increase the magnetic flux linked from an external excitation source by increasing the effective area. Secondly, multiple connections between the longest edges have been realized by additional transversal paths in order to distribute the circulating currents, and hence Lorentz forces, near the free end of the

cantilever to maximize the induced amplitude of vibration.

The choice of the width and the reciprocal distance of the transversal paths have been dictated by the constraint of granting an equal distribution of the circulating current in each path. To this purpose, AC electromagnetic simulations with COMSOL have been run to verify the designed geometry. In particular, a unit current density has been forced in the complete path and the current intensity in each transversal path has been computed. Figure 8 shows the results of the simulation where the colormap plot on the geometry represents the current density distribution. The table reports the value of the current I in each transversal path, labeled from “1” to “4”. As it can be observed, the evaluated currents are approximately equal.

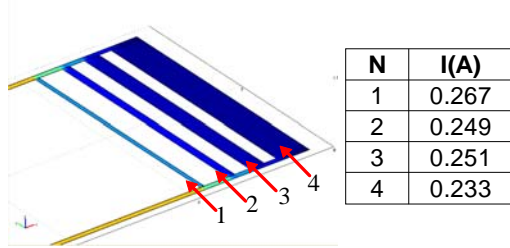


Figure 8. Results of the simulation.

For the design of the MEMS resonators, cantilevers and clamped-clamped beams have been considered. First order approximations of the resonance frequencies of the two types of the structures, expressed in hertz, have been derived by the relation:

$$f_{ris} = \alpha \frac{h}{L^2} \sqrt{\frac{E}{\rho}} \quad (5)$$

where h is the thickness, L is the length, E is the Young's modulus, ρ is the mass density, and α is a constant which assumes the value of 0.1616 for the cantilever beam and 1.0284 for the clamped-clamped beam.

The MEMS resonators have been fabricated employing a bulk-micromachining process based on a BESOI (Bond and Etch back - Silicon On Insulator) offered by the CNM (Centro Nacional de Microelectronica) in Barcelona, Spain. Figure 9 shows the layers of the process which allows for one layer of polysilicon and two layers of metals.

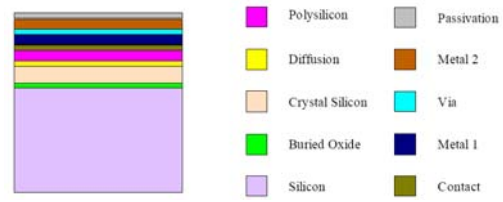


Figure 9. Layers of the CNM bulk micromachining process.

Mechanical eigenfrequency simulations have been run to confirm the first-order analysis and to correct the estimations by including the effects of the thickness of the main process layers. Figure 10 shows a simulation for a cantilever beam with dimensions of 1500 x 700 x 15 μm for which a resonance frequency of 9404 Hz has been computed, while the value given from (5) is 9204 Hz.

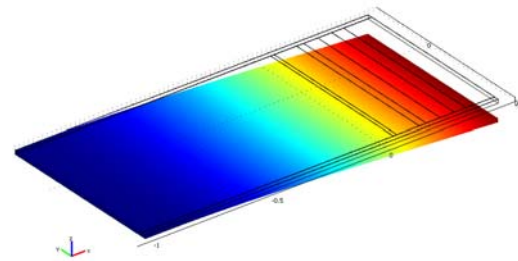


Figure 10. Results of the eigenfrequency simulation.

4.2 Experimental results for MEMS resonators

Figure 11 shows a picture of one of the realized MEMS resonators. In particular, this device is composed of four cantilever beam resonators. An on-chip multi-turn coil and a single-turn coil with conductive paths running along the edges of the cantilevers have been implemented. Each of the cantilevers can be contactless excited adopting a proper arrangement of external coils and magnets and exploiting the on-chip conductive paths.

Figure 12 reports a schematic diagram of the experimental setup adopted, where the resonator is located on a holder substrate housing a magnet on the opposite side.

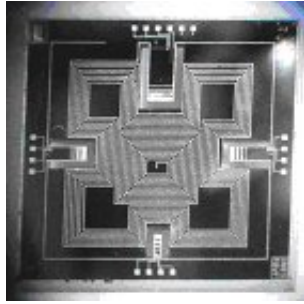


Figure 11. Picture of the fabricated MEMS.

The single-turn coil on the MEMS is connected to an external coil (C2) faced to the coil (C1) used for excitation. C1 is driven by an AC current I_e , and the electromotive force induced on C2 by the varying flux of C1 generates a current I in the single-turn coil on the MEMS. The current I interacts with the radial component B_r of the static magnetic field generated by the magnet and a Lorentz force F_z acting on the MEMS is generated, which sets the resonator into flexural vibrations.

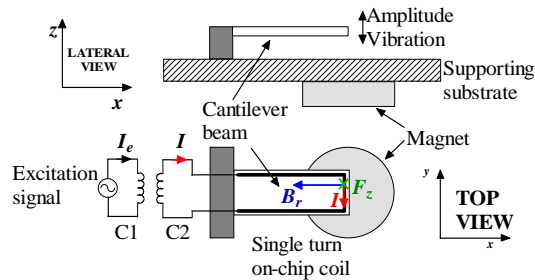


Figure 12. Schematic diagram of the experimental setup for MEMS resonators.

Subsequently, the coil C1 has been driven with an AC current of 200 mA rms and the vibrations of the MEMS have been measured with the optical system. Figure 13 shows the typical measured frequency response of the displacement-excitation ratio. From the reported curves, a resonance frequency of 8390 Hz can be observed, which is in good agreement with the prediction of the simulations.

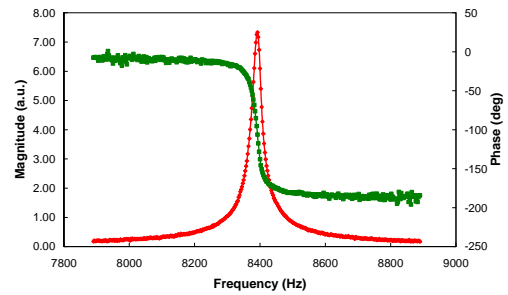


Figure 13. Frequency response of the displacement-excitation ratio of the investigated cantilever by means of contactless electromagnetic excitation.

5. Conclusions

This work has investigated the possibility of contactless exciting miniaturized and MEMS resonators by means of electromagnetic techniques. The principle relies on no specific magnetic property of the structure except electrical conductivity. In particular, FEM simulations have confirmed the theoretical predictions of the model of the excitation principle which has been tested experimentally on miniaturized resonators. Subsequently, by studying the effects of the downscaling of the dimensions of the structures, the principle has been implemented in the design of optimized MEMS resonators. Experimentally, the principle has been verified on one of the designed resonators, namely a cantilever beam. At present, the experimental activity is investigating the possibility of extending the principle to vibration readout, which has been already demonstrated to be effective on millimetre-size sensors [9]. In this context, COMSOL simulations will be exploited to analyze the key geometric and electrical parameters of the resonators which can lead to the realization of MEMS resonant sensors that can be contactless excited and detected. Though no specific measurand quantity has been addressed, the investigated principle can be adopted to excite contactless sensors operating on short-range excitation distance of the order of 1 cm. The sensors can be applied to the measure of any physical or chemical quantity that can cause a predictable shift in the resonance frequency of the structure.

6. References

1. M. R. Gibbs, E. W. Hill, P. J. Wright, Magnetic materials for MEMS applications, *Journal of Applied Physics D: Applied Physics* **37**, 237-244, (2004).
2. S. Baglio, L. Latorre, P. Nouet, Resonant magnetic field microsensors in standard CMOS technology, *Proceedings of IMTC*, 452-457, (1999).
3. E. K. Reichel, B. Weiß, C. Riesch, A. Jachimowicz, B. Jakoby, A novel micromachined liquid property sensor utilizing a doubly clamped vibrating beam, *Proc. XX Eurosensors*, 17-20, (2006).
4. F. Lucklum, P. Hauptmann, N. F. de Rooij, Magnetic direct generation of acoustic resonance in silicon membranes, *Measurement and Science Technology*, **17**, 719-726, (2006).
5. A. C. Stevenson, C. R. Lowe, Magnetic-acoustic-resonator sensors (MARS): a new sensing methodology, *Sensors and Actuators A*, **72**, 32-37, (1999).
6. C. De Angelis, V. Ferrari, D. Marioli, E. Sardini, M. Serpelloni, A. Taroni, Magnetically induced oscillations on a conductive cantilever for resonant microsensors, *Sensors and Actuators A*, **135**, 197-202, (2007).
7. M. Baù, V. Ferrari, D. Marioli, E. Sardini, M. Serpelloni, A. Taroni, Contactless electromagnetic excitation of resonant sensors made of conductive miniaturized microstructures, *Sensors and Actuators A*, **148**, 44-50, (2008).
8. M. Baù, V. Ferrari, D. Marioli, A. Taroni, Cost-effective system for the characterization of microstructures vibrating in out-of-plane modes, *Sensors and Actuators A*, **142**, 270-275, (2008).
9. M. Baù, V. Ferrari, D. Marioli, E. Sardini, M. Serpelloni, A. Taroni Contactless Excitation and Readout of Passive Sensing Elements Made by Miniaturized Mechanical Resonators, *Proc. IEEE Sensors*, 36-39, (2007).